institut für thermodynamik ift

Technische Universität Braunschweig

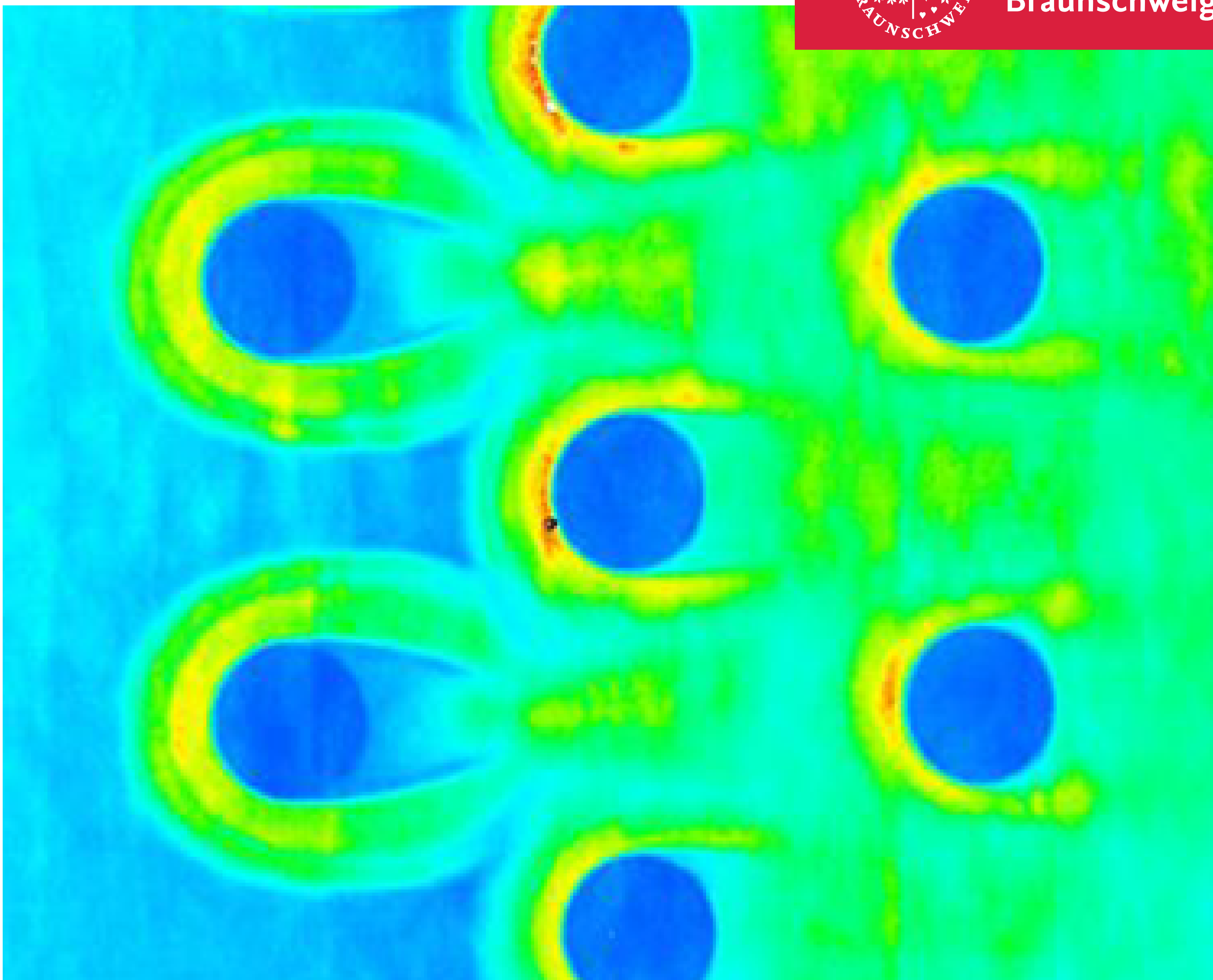

Adaptive Controller Design for Refrigeration Cycle Using the Natural Refrigerant CO_2

Masterarbeit

Autor: Julius Martensen
Betreuer: Dipl. Ing. Michael Nöding
Prüfer: Prof. Dr.-Ing. Jürgen Köhler

August 16, 2017

Technische Universität Braunschweig

Institut für Thermodynamik

institut für thermodynamik ift

Prof. Dr.-Ing. Jürgen Köhler
Hans-Sommer-Str. 5
D-38106 Braunschweig
Tel.: +49 (531) 391-2627
Fax: +49 (053) 391-7814
E-Mail: J.Koehler@tu-bs.de
Braunschweig, 29.09.2014

Vorlesungsankündigung

Im Wintersemester 14/15 werden die folgenden Lehrveranstaltungen abgehalten:

Thermodynamik

Prof. Dr. J. Köhler/Dipl.-Ing. M. Buchholz

2519023	**Die allererste Vorlesung ist am Donnerstag, 23.10.2014 von 15.00 bis 16.30 Uhr im AM**					
	2V	Vorlesung	MI	15:00 - 16:30	AM	29.10.2014
	1V	Vorlesung	DO	14:55 - 15:40	AM	23.10.2014
2519029	1Ü	Übung	DO	15:50 - 16:55	AM	23.10.2014
2519004	2S	Seminargruppe	FR	08:15 - 11:15	ZI 24.1 - ZI 24.3	31.10.2014

Thermodynamik der Gemische

Prof. Dr. J. Köhler/Dr. G. Raabe

2519038	2V	Vorlesung	FR	11:30 - 13:00	PK 4.1	24.10.2014
2519039	1Ü	Übung	FR	13:10 - 13:55	PK 4.1	24.10.2014

Modellierung thermischer Systeme in Modelica

Prof. Dr. J. Köhler/Dr. W. Tegethoff

2519006	2V	Vorlesung	nach Absprache	HS 5.1	Beginn: siehe gesonderter Aushang
2519008	1Ü	Übung	nach Absprache	HS 5.1	Beginn: siehe gesonderter Aushang

Objektorientierte Simulationsmethoden in der Thermo- und Fluiddynamik

Prof. Dr. J. Köhler/Dr. W. Tegethoff

2519011	2V	Vorlesung	nach Absprache	HS 5.1	Beginn: siehe gesonderter Aushang
2519012	1Ü	Übung	nach Absprache	HS 5.1	Beginn: siehe gesonderter Aushang

Seminar für Thermodynamik

Prof. Dr. J. Köhler/Wiss. Mitarbeiter N.N.

2519024	2S	Seminar	MO	13:15-14:45	HS 5.1	

Fahrzeugklimatisierung

Prof. Dr. J. Köhler/Dr. N. Lemke

2519003	2V	Vorlesung	DI	16:45 - 18:15	HS 5.1	Beginn: siehe gesonderter Aushang
2519034	1Ü	Übung	siehe gesonderter Aushang			Beginn: siehe gesonderter Aushang

Prof. Dr.-Ing. Jürgen Köhler

Eidesstattliche Erklärung

Hiermit erkläre ich eidesstattlich, dass ich diese Arbeit eigenständig angefertigt und keine anderen als die angegebenen Hilfsmittel verwendet habe.

Braunschweig den August 16, 2017

Contents

List of Figures

1 Introduction

1.1 Motivation

The great motivational Speak follows in this section.

Hier schon folgende Quellen erwÃ¤hnen:

[7]

1.2 Literature Review

The great literature review follows in this section.

2 Thermodynamic Statement of the Problem

The following chapter gives a brief introduction to the needed basics from a thermodynamic point of view.

In the first section the system is described from a technical perspective followed by a general thermodynamic process model.

Afterwards the model used for simulating the system in Dymola is explained.

At last the problem motivating this thesis is formulated in the context of thermodynamics.

2.1 Process Description

2.2 Problem Statement

The aim of enginnering thermodynamics is - as stated earlier in Chap. 1 - to understand and optimize the behaviour of technical systems used for energy transformation and transportation. Hence, a connection to the field of optimal control is a logical extension to maximize the efficiency. As described in sec. 2.1 the systems states are general interconnected by both physical components and physical phenomena. In the following section the coupling due to physical phenomena will be investigated.

The process can be divided in three basic processes:

- Isobaric process with heat supply
- Adiabatic isenthalpic process
- Isentropic process with exchange of (mechanical) work

We can characterize these processes using the First Law of Thermodynamics in differential form, see e.g. [12, p.25]:

$$\begin{aligned} du &= d\left(h - pv\right) \\ &= dh - vdp - pdv \\ &= \delta q + \delta w_{diss} - pdv \end{aligned} \tag{2.1}$$

Which states that the change in inner energy $u \in \mathbb{R}$ is equal to the sum of heat $\delta Q \in \mathbb{R}$ and dissipated work $\delta w_{diss} \in \mathbb{R}$ minus the pressure-volume work, depending on the pressure $p \in \mathbb{R}^+$ times the change in specific volume $v \in \mathbb{R}^+$. The internal energy can be related to the specific enthalpy $h = u + pv \in \mathbb{R}$.

The Second Law of Thermodynamics as formulated by Gibbs [11, p.59] is given by:

$$\begin{aligned} Tds &= du + pdv \\ &= d(h - pv) + pdv \\ &= dh - vdp \end{aligned} \tag{2.2}$$

Defining two independent to be state variables the specific volume v and temperature T and substitute Eq.2.1 in Eq.2.2:

$$\begin{aligned} Tds &= du + pdv \\ &= \delta q + \delta w_{diss} \end{aligned} \tag{2.3}$$

Since the total differential of the inner energy is given by

$$du = \left(\frac{du}{dT}\right)_v dT + \left(\frac{du}{dv}\right)_T dv \tag{2.4}$$

Substitute Eq. 2.4 in 2.3 while using the definition for the specific heat capacity at constant volume $c_V = \left(\frac{\partial u}{\partial T}\right)_v \in \mathbb{R}^+$ holds:

$$\begin{aligned} Tds &= \left(\frac{\partial u}{\partial T}\right)_v dT + \left(\frac{\partial u}{\partial v}\right)_T dv + pdv \\ &= c_v dT + \left[p + \left(\frac{\partial u}{\partial v}\right)_T\right] dv \end{aligned}$$

Using the relation [11, p.375] $T\left(\frac{\partial s}{\partial v}\right)_T = \left(\frac{\partial u}{\partial v}\right)_T + p$ and the Maxwell Relation $\left(\frac{\partial s}{\partial v}\right)_T = \left(\frac{\partial p}{\partial T}\right)_v = \frac{\beta}{\kappa}$ the equation becomes:

$$\begin{aligned} Tds &= \left(\frac{\partial u}{\partial T}\right)_v dT + \left(\frac{\partial u}{\partial v}\right)_T dv + pdv \\ \delta q &= c_v dT + T\frac{\beta}{\kappa} dv \end{aligned} \tag{2.5}$$

The coefficient of thermal expansion at constant pressure $\beta \in \mathbb{R}$ is defined by $\frac{1}{v}\left(\frac{dv}{dT}\right)_p = \beta$ and the compressibility $\kappa = \left(\frac{\partial v}{\partial p}\right)_T \in \mathbb{R}^+$ substitute the differential change of pressure due to temperature at constant volume via the chain rule.

Eq. 2.5 states that the exchange of heat in the isobaric process results in a change of specific volume and temperature.

The massflow $\frac{dm}{dt} = \dot{m} \in \mathbb{R}$ from A to B through a throttle can be described by a function of the density $\rho = \frac{1}{v} \in \mathbb{R}^+$, the effective area $A_{eff} \in \mathbb{R}^+$ and the difference in pressure

$$\dot{m} = A_{eff}\sqrt{2\rho_A \left(p_A - p_B\right)} \tag{2.6}$$

we can directly relate the difference pressure $p_A - p_B = \Delta p > 0$ to the exchange of heat. Assume a constant mass flow, a constant effective Area and a constant pressure niveau p_B due to perfect controller of the system, the energetic coupling between fan and pressure can be seen. If heat is added before A as described by Eq. 2.5 the Temperature in A will be influenced as well the pressure due to the change in the specific volume and therefore the density via Eq.2.6.

The isenthalpic, adiabat throttling process can be described by the Joule-Thomson Coefficient [11, p.387]. The equation relates the change in temperature and pressure to each other via

$$\begin{aligned} \left(\frac{\partial T}{\partial p}\right)_h &= -\frac{1}{c_p}\left(\frac{\partial h}{\partial p}\right)_T \\ &= \frac{v}{c_p}\left(T\beta - 1\right) \end{aligned} \tag{2.7}$$

Where $c_p = \left(\frac{\partial h}{\partial T}\right)_p \in \mathbb{R}^+$ is the specific heat at constant pressure which relates the change in entropy due to a change in temperature. Eq. 2.7 and Eq. 2.6 relate the change in pressure via variation of the effective Area to the change in temperature.

Eq. 2.5, 2.6 and 2.7 show the thermodynamic coupling of the system. They are highly nonlinear and give an ideal coupling for the quasi stationary processes and the choosen states pressure and temperature. Since both couplings take effect at the same time, a reasonable estimation of the process trajectory is difficult.
An important fact is that none of the equations above depend explicitly on the time. All coefficients above are functions of the thermodynamic states p, v, T, s. Assuming quasi stationary behaviour of the system for every coefficent $c \in \left\{\beta, \kappa, c_v, c_p\right\}$ they can be related to the static gain of the couplings.

Further physical phenomena interconnecting the system can be related to hydraulic capacity, hydraulic inductivity

3 Control Theoretic Model and Problem Statement

The following chapter explains the

3.1 Basics of Control Theory

A general nonlinear, dynamical system Σ can be described [1]

$$\begin{aligned} \dot{\boldsymbol{x}} &= \boldsymbol{f}\left(\boldsymbol{x}, \boldsymbol{u}, t\right) \\ \boldsymbol{y} &= \boldsymbol{h}\left(\boldsymbol{x}, \boldsymbol{u}, t\right) \end{aligned} \tag{3.1}$$

Where $t \in \mathbb{R}^{+}$ is the time, $\boldsymbol{x} \in \mathbb{R}^{n_x}$ is called the state vector, or states, and $\boldsymbol{u} \in \mathbb{R}^{n_u}$ the input vector, or inputs, of the system. The output $\boldsymbol{y} \in \mathbb{R}^{n_y}$ of the system is described by the functions$\boldsymbol{h}$: $\mathbb{R}^{n_x}, \mathbb{R}^{n_u}, \mathbb{R}^{+} \mapsto \mathbb{R}^{n_y}$ and the evolution of the system over time is given by $\boldsymbol{f}: \mathbb{R}^{n_x}, \mathbb{R}^{n_u}, \mathbb{R}^{+} \mapsto \mathbb{R}^{n_x}$.

The System given by Eq. 3.1 can be used to describe almost every natural or technical system. Due to several reasons, e.g. controller design, measurements, modelling issues and errors, most technical applications simplify the model by assuming linear, time invariant (LTI) behaviour. The LTI system is represented by a set of first-order differential equations [9] called state space representation:

$$\begin{aligned} \dot{\boldsymbol{x}} &= \boldsymbol{A}\,\boldsymbol{x} + \boldsymbol{B}\,\boldsymbol{u} \\ \boldsymbol{y} &= \boldsymbol{C}\,\boldsymbol{x} + \boldsymbol{D}\,\boldsymbol{u} \end{aligned} \tag{3.2}$$

The state matrix $\boldsymbol{A} \in \mathbb{R}^{n_x \times n_x}$ describes the influence of the current states, the input matrix $\boldsymbol{B} \in \mathbb{R}^{n_x \times n_u}$ the influence of the current input on the future states and output. The output is given by the output matrix $\boldsymbol{C} \in \mathbb{R}^{n_y \times n_x}$ and the feedthrough matrix $\boldsymbol{D} \in \mathbb{R}^{n_y \times n_u}$.

Both Eq. 3.1 and Eq. 3.2 are able to generate a variety of different controllers, see e.g. [1],[9], [10]. The ability to design controller via state space methods is connected to a high information content about (physical) parameters and equations or in form of measurement data.

Hence a more compressed form is commonly used to design controller for most technical and industrial applications. The transfer function matrix [9, p.20] $\boldsymbol{G} \in \mathbb{C}^{n_y \times n_u}$ can be derived via the Laplacetransform of Eq.3.2:

$$G = C\left(sI - A\right)^{-1} B + D \tag{3.3}$$

The transfer function matrix consist of single transfer functions $g_{ij}(s)$ $, i \leq n_y, j \leq n_u$ and maps the transformed input of a system directly to its transformed output. It describes the relationship between input and output directly and is hence a compact form of describing the behaviour of LTI systems. To control a system with two outputs in every wanted direction a necessary condition is given by $n_y \leq n_u$. It is assumed that all following systems suffice dim $G = n_y \times n_y$.

3.2 Feedback Control in Presence of Uncertain Signals

The aim of control theory is to manipulate a systems trajectory via its inputs in such a way, that a desired output is reached and maintained. To do this, several techniques can be used. Most commonly the systems desired output, the setpoint y_r, is compared to the actual output of the system y via a feedback loop. The result of this comparison is called the error $e \in \mathbb{R}^{n_y}$. This signal is fed into the controller $K \in \mathbb{C}^{n_y \times n_y}$ and the result is used as an input for the system. This approach is called feedback control, see e.g. [3], with a single degree of freedom controller.

A variation of this approach is to use a weighted set point and output signal to generate the input. The pair of weighting matrices K_r for the setpoint and K_y for the output is called a two degree of freedom controller. The structure of such a controller design is shown in Fig. 3.1.

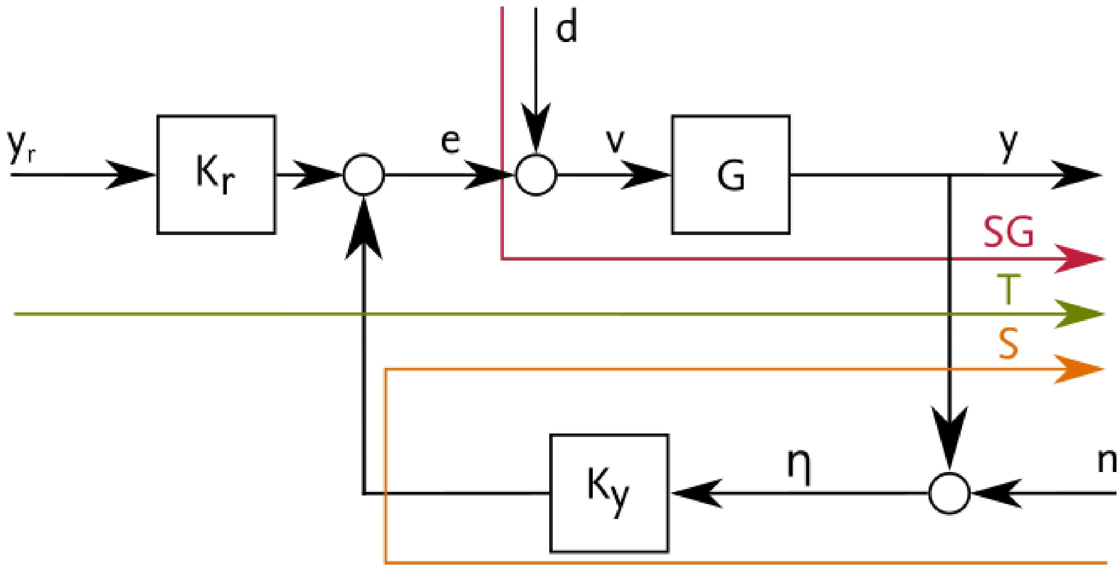

Figure 3.1: Two Degree of Freedom Feedback Control

In Fig. 3.1 other signals are added as well.The disturbances $d \in \mathbb{R}^{n_y}$ are acting on the weighted error. The signal $v \in \mathbb{R}^{n_y}$ is the disturbed input of the plant. $\eta \in \mathbb{R}^{n_y}$ is the plants output without measurement noise which will be referred to as real output. The measurement noise is given by

$\boldsymbol{n} \in \mathbb{R}^{n_y}$. The superposition of noise and real output is $\boldsymbol{y}$ which will be referred to simply as output. The closed loop transfer function is given by:

$$\boldsymbol{y} = \left[\boldsymbol{I} - \boldsymbol{G}\boldsymbol{K}_y\right]^{-1} \left[\boldsymbol{G}\boldsymbol{K}_r\boldsymbol{y}_r + \boldsymbol{n} + \boldsymbol{G}\boldsymbol{d}\right] \tag{3.4}$$

Eq. 3.4 relates the output of a system to the influences of set point, disturbances and measurement noise. Rewriting the equation as:

$$\boldsymbol{y} = \boldsymbol{T}\boldsymbol{y}_r + \boldsymbol{S}\left[\boldsymbol{n} + \boldsymbol{G}\boldsymbol{d}\right] \tag{3.5}$$

defines the Sensitivity Function $\boldsymbol{S} = \left[\boldsymbol{I} - \boldsymbol{G}\boldsymbol{K}_y\right]^{-1} \in \mathbb{C}^{n_y \times n_y}$ which relates the influences of measurement noise and load disturbance to the systems outputs. The Complementary Sensitivity Function $\boldsymbol{T} = \left[\boldsymbol{I} - \boldsymbol{G}\boldsymbol{K}_y\right]^{-1} \boldsymbol{G}\boldsymbol{K}_r \in \mathbb{C}^{n_y \times n_y}$ describes the response to the reference signal.Both Functions play an important role in the investigation of the systems Robustness and are connected to each other via $\boldsymbol{T} = \boldsymbol{S}\boldsymbol{G}\boldsymbol{K}_r$.

3.3 Robustness and Stability of Feedback Control Systems

Robustness refers in general to the stability of the system in presence of uncertainties and has been studied extensively, see e.g. [13],[?], [?]. To give a better understanding of the relevant points of the subject both SISO and MIMO cases are presented.

For any given SISO system with a transfer function $g : \mathbb{R} \mapsto \mathbb{C}$ we see from Eq. 3.4 that the behaviour of the output with respect to measurement noise and disturbances is strongly dependent on the sensitivity function. A necessary condition for the system to reach the reference is that disturbance and noise are attenuated near the steady state. Furthermore the destabilizing effect due to uncertain signals can be quantified via the maximum of the sensitivity function. Therefore the Maximum Sensitivity is defined as:

$$\begin{aligned} M_S &= \max_{\omega} |S| \\ &\geq \left| \frac{1}{1 - g\,k_y} \right| \end{aligned} \tag{3.6}$$

With Eq. 3.6 an upper boundary on the gain can be found and be used as a measure of robustness of the closed loop [3, p.323 ff.]. The maximum sensitivity is also connected to the nyquist stability and the stability margin of a system via:

$$\begin{aligned} M_S &= \frac{1}{s_M} \\ &= \frac{1}{1 - \max_{\omega} |g\,k_y|} \end{aligned} \tag{3.7}$$

Or rearranged to be:

$$\max_{\omega} |g\, k_y| = 1 - s_M \tag{3.8}$$

Due to Eq. 3.7 the maximum gain of the open loop is limited by the maximum sensitivity. Hence, the critical point is only encircled iff the maximum sensitivity is zero. Hence the system is only stable in the sense of the Nyquist Criterion if the maximum sensitivity is sufficiently small.

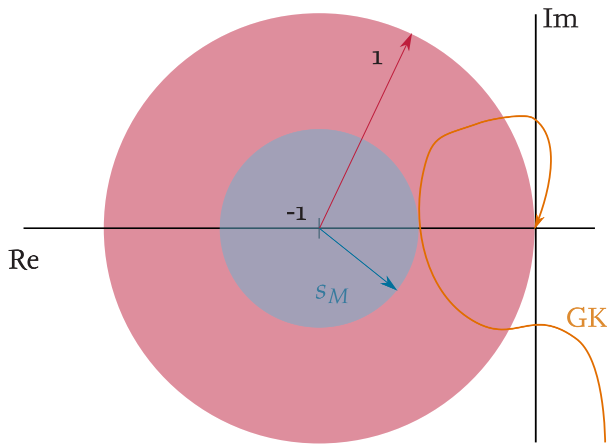

Figure 3.2: Maximum Sensitivity

While the maximum sensitivity is well definied for SISO systems, a MIMO system requires a more general approach due to the interconnection of the systems out- and inputs. A general condition is given by the Small Gain Theorem [?, p.150 ff.]. The theorem states, that a given feedback system is stable iff the open loop transfer function matrix is stable and its sufficient conditioned matrix norm is less than 1 over all frequencies.

$$\|\boldsymbol{GK}_y\| < 1\ \forall\omega \tag{3.9}$$

Eq. 3.9 can be used with several matrix norms and can be viewed as an MIMO Interpretation of the Nyquist Criterion.

For further robustness analysis, the concept of singular values has to be investigated. The singular value decomposition, see e.g. [?, p.144 f.],states that any matrix $\boldsymbol{G} \in \mathbb{C}^{n_a \times n_b}$ can be factorized such that

$$\boldsymbol{G} = \boldsymbol{U}\boldsymbol{\sigma}\boldsymbol{V}^* \tag{3.10}$$

Where as $\boldsymbol{U} \in \mathbb{C}^{n_a \times n_a}$ and $\boldsymbol{V} \in \mathbb{C}^{n_b \times n_b}$ are unitary matrices representing the left and right eigenvectors of matrix. The matrix $\boldsymbol{\sigma} \in \mathbb{C}^{n_a \times n_b}$ is a rectangular, diagonal matrix consisting of the singular values $\sigma \in \mathbb{C}$ of $\boldsymbol{G}$. A practical point of view suggest a rotation of any given input vector via $\boldsymbol{V}^*$, distributing the magnitude of the input over the columns of $\boldsymbol{\sigma}$, where they are scaled according to the magnitude of the corresponding singular value. Then the scaled and rotated vector is once again rotated by $\boldsymbol{U}$ and distributed over the output vector.

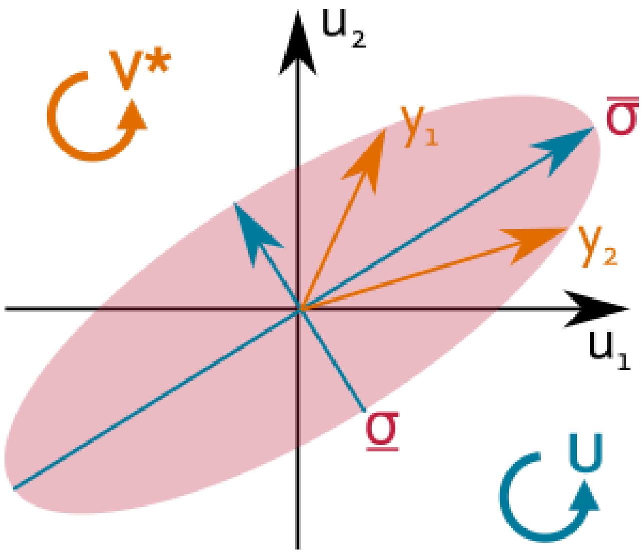

Figure 3.3: Graphical Interpretation of the Singular Value Decomposition

An example of this process is illustrated in Fig. 3.3 for a system with two inputs u_1, u_2 and two outputs y_1, y_2. The output is bounded by the ellipsoid described by the maximum singular value $\overline{\sigma}$ and the minimum singular value $\underline{\sigma}$. The orientation and the magnitude of the outputs change depending on the frequency but will never exceed these limits. The singular values of a matrix are hence representing the highest possible gain for any given input if $\boldsymbol{U} = \boldsymbol{V}^* = \boldsymbol{I}$. With that, the induced 2-Norm for a matrix can be defined as:

$$\begin{aligned} \|\boldsymbol{G}\|_2 &= \frac{\|\boldsymbol{G}\boldsymbol{u}\|_2}{\|\boldsymbol{u}\|_2} \\ &= \max \sqrt{\lambda\left(\boldsymbol{G}^*\boldsymbol{G}\right)} \\ &= \overline{\sigma} \end{aligned} \tag{3.11}$$

3.4 Gain Scheduling

4 Process Models and System Identification

4.1 First Order Time Delay Model

As discussed earlier system identification enables the user to use various methods to process information to derive a suitable dynamical model.To ensure a deterministic, robust and simple controller an identification based on analogous models is choosen. The reasons for this approach are based on the variety of the process itsself as well as the algorithms used for determination of the controller parameter, see [2], [5].

The model structure used in the scope of the work is a given by the transfer function

$$\hat{G} = \frac{\hat{K}}{\hat{T}s + 1} e^{-\hat{L}s} \tag{4.1}$$

Eq. 4.1 describes the function $\hat{G} : \mathbb{C} \mapsto \mathbb{C}$ in the s-plane and is called a first order time delay (FOTD) or first order plus deadtime (FOPDT) model, [2, p.16], [5, p.20], [8], The model gain $\hat{K} \in \mathbb{R}$ is the steady state gain of the system, a model time constant $\hat{T} \in \mathbb{R}^{+}$ and a model time delay $\hat{L} \in \mathbb{R}^{+}$ describe the dynamic gain and phase. Its represenation as a differential equation is given to be

$$\hat{T} \frac{dy}{dt} + y = \hat{K} \, \sigma(t - \hat{L}) \; u \tag{4.2}$$

With the general solution for a step response acting on Eq.4.2 is

$$y = \hat{K} \left(1 - e^{-\frac{t-\hat{L}}{\hat{T}}}\right) \sigma(t - \hat{L}) \; u \tag{4.3}$$

The Heavyside step function $\sigma(t) : \mathbb{R} \mapsto \mathbb{R}$ is defined as

$$\sigma(t) = \begin{cases} 0, \; t < 0 \\ 1, \; t \geq 0 \end{cases} \tag{4.4}$$

and hence models the delay acting on the connection between the output and the input. It is worth noting that in the special case of a SISO system a delay acting on the systems input or output is mathematical equivalent. However, for a given MIMO system model it can be of importantance to define where the delay intervenes.

An important characteristic with respect to the time behaviour of the process is given by the normalized time τ, $[0 \geq \tau \geq 1]$ [, p.16]AstromPID

$$\tau = \frac{\hat{L}}{\hat{L} + \hat{T}} \tag{4.5}$$

Eq. 4.5 gives the ratio of the delay and the delay and the time constant, called average residence time. It can be used as a rating regarding the difficulty of controlling the process, since a high normalized time indicate a delay dominance and hence a very difficult process to control.

Since the process model is of upmost interest for the overall process, a detailed investigation of its properties is conducted. This detailed description is started by investigating the model gain over the frequency. It is conventional to substitute the complex varibales with the complex frequency $s = j\,\omega$. The gain of the process modell is hence given by:

$$\begin{aligned} |\hat{G}| &= \left| \frac{\hat{K}}{\hat{T}\, j\omega + 1}\, e^{-\hat{L}\, j\omega} \right| \\ &= \left| \frac{\hat{K}}{\hat{T}\, j\omega + 1} \right| \quad \underbrace{\left| e^{-\hat{L}\, j\omega} \right|}_{\left|cos(\hat{L}\omega) + j\; sin(\hat{L}\omega)\right| = 1} \\ &= \left| \frac{\hat{K}}{\hat{T}\, j\omega + 1} \right| \end{aligned} \tag{4.6}$$

Eq.4.6 shows that the gain over the frequency of FOTD model is equal to a first order system with the same gain and time constant. The effect of the time delay is cancelled due to the use of Euler's identity, which can be interpreted as an orthonormal roation in the complex plane by an angle $\hat{L}\omega$ around the orign.

The systems phase can be described as

$$\begin{aligned} \hat{\varphi} &= \arg\left(\hat{G}\right) \\ &= \arg\left(\frac{\hat{K}}{\hat{T}\, j\omega + 1}\, e^{-\hat{L}\, j\omega} \right) \\ &= \arg\left(\frac{\hat{K}}{\hat{T}\, j\omega + 1} \right) + \arg\left(e^{-\hat{L}\, j\omega} \right) \\ &= \arg\left(\frac{\hat{K}}{\hat{T}\, j\omega + 1} \right) - \hat{L}\omega \end{aligned} \tag{4.7}$$

From Eq.4.7 the effect of the time delay follows directly. It imposes a negative shift in phase proportional to the frequency on the system.

Defining an error between the real, unknown system and the FOTD model requires the following identities of a general transfer function:

$$
\begin{aligned}
G &= \frac{\sum_{i=0}^{n} a_i s^i}{\sum_{k=0}^{m} b_k s^k} \\
&= \frac{\prod_{i=0}^{n} \left(s^i - z_i\right)}{\prod_{k=0}^{m} \left(s^k - p_k\right)}
\end{aligned}
\tag{4.8}
$$

Eq.4.8 shows the identities of a transfer function given as a polynomial in s and its equivalent representation as a product of linear factor, see LUNZE1,p.269 ff. . The linear factorization consists of its zeros $z_i \in \mathbb{C}$ and poles $p_k \in \mathbb{C}$. Both identities will be usefull due to the different propoerties of the gain and phase. Additionally it is assumed that the first order dynamics have been idealy identified. Hence, the error depends only on dynamics of higher order.

Further investigation requiere the relative difference of the FOTD model with respect to the The relative error in Gain $\Delta_K \in \mathbb{C}$ can therefore described as

$$
\begin{aligned}
\Delta_K &= \left| \frac{\hat{G}}{G} \right| \\
&= \underbrace{\left| \frac{\hat{K}}{\hat{T}\, j\omega + 1} \frac{(1 - p_0)\,(s - p_1)}{1 - z_0} \right|}_{\approx 1} \left| \frac{\prod_{k=2}^{m} \left(s^k - p_k\right)}{\prod_{i=1}^{n} \left(s^i - z_i\right)} \right| \\
&\approx \left| \frac{\prod_{k=2}^{m} \left(s^k - p_k\right)}{\prod_{i=1}^{n} \left(s^i - z_i\right)} \right|
\end{aligned}
\tag{4.9}
$$

From Eq.4.9 two important conclusions can be conducted. First, the error is small near the steady state iff the first order dynamics are estimated correctly. The steady state model is even error free, iff the true gain can be identified. Secondly, the error will increase dramaticly for higher order dynamics since the model is not able to project these frequencies in an adequat manner. Another source of error can be found in low order zeros of the system, which will result in an infinite error of the gain.

Likewise, the relative error in phase $\Delta_\varphi \in \mathbb{C}$ is given as:

$$
\begin{aligned}
\Delta_\varphi &= \arg\left(\frac{\hat{G}}{G} \right) \\
&= \arg\left(\underbrace{\frac{\hat{K}}{\hat{T}\, j\omega + 1} \frac{(1 - p_0)\,(s - p_1)}{1 - z_0}}_{\approx 1} \frac{\prod_{k=2}^{m} \left(s^k - p_k\right)}{\prod_{i=1}^{n} \left(s^i - z_i\right)} e^{-\hat{L}\, s} \right) \\
&= -L\,\omega + \arg\left(\frac{\prod_{k=2}^{m} \left(s^k - p_k\right)}{\prod_{i=1}^{n} \left(s^i - z_i\right)} \right)
\end{aligned}
\tag{4.10}
$$

Eq. 4.10 gives an important insight to the function of the time delay. It compensates for the higher order dynamics in phase, effectively reducing the error in phase.

Of course the chance to identify the first order dynamics right are effectively zero. But since heat transfer is described as a first order equation, called Newton's Law of cooling HIER ZITIEREN, it is valid to assume the higher order dynamics to be small. Furthermore it can be assumed to be the time dominant process of the cycle. Hence the valve, which is normally modeled as a second order system can be described as a first order system as well, since it is acting in much faster timescales.

4.2 Integral Fitting Approach

The first algorithm to estimate the parameter of the model is based on inherent knowledge of the time behaviour of the model. These properties described in the section can be found in LUNZE, FEDELE, u.a. and are part of mostly any undergraduate course in control theory. The experiment providing the needed data is a step repsonse around the working point. The algorithm depends on the collected data of the input, the output and the time. It processes the data by evaluating several numerical integrals and connects the outcomes to the process parameters.

At first, the difference between the settling value of the ouput, $y(\infty)$, and the current value, $y(t)$, is computed over time

$$
\begin{aligned}
\int_0^\infty y(\infty) - y(t)\, dt &= \int_0^\infty y(\infty) - \hat{K}\ \left(1 - e^{-\frac{t-\hat{L}}{\hat{T}}}\right)\ \sigma(t-\hat{L})\, dt \\
&= \hat{K} \int_0^{\hat{L}} \sigma(t)\, dt + \hat{K} \int_0^\infty e^{-\frac{t}{\hat{T}}}\, dt \\
&= \hat{K}\, \hat{L} + \hat{K} \left(-\hat{T} e^{-\frac{t}{\hat{T}}}\right) \Bigg|_0^\infty \\
&= \hat{K}\ (\hat{T} + \hat{L}) \\
&= \hat{K}\, \hat{T}_{ar}
\end{aligned}
\tag{4.11}
$$

In Eq.4.11 the average residence time $\hat{T}_{ar} \in \mathbb{R}^+$ is calculated from the integral. To simplify the equation above the linearity of the integral has been employed. Additionally the properties of the Heavyside function enabled a change in the lower boundary, hence the simplification.

Further exploitation of Eq. 4.3 leads to [width=]../Graphics/TEST.svg

Figure 4.1: Area Based Interpretation of the Integral Fitting Approach

$$\begin{aligned}\int_0^{\hat{T}_{ar}} y(t)\,dt &= \int_0^{\hat{T}_{ar}} \hat{K}\,\left(1-e^{-\frac{t-\hat{L}}{\hat{T}}}\right)\,\sigma(t-\hat{L})\,dt\\ &= \int_{\hat{L}}^{\hat{T}_{ar}} \hat{K}\,\left(1-e^{-\frac{t}{\hat{T}}}\right)\,dt\\ &= \hat{K}\left(t+\hat{T}e^{-\frac{t}{\hat{T}}}\right)\Bigg|_{\hat{L}}^{\hat{T}_{ar}}\\ &= \frac{\hat{K}}{e}\hat{T}\end{aligned} \tag{4.12}$$

At last, the gain $\hat{K}$ has to be computed. With the common definition, e.g. given in LUNZE1, the parameter can be computed using

$$\hat{K} = \lim_{t\mapsto\infty} \frac{y(t)-y(0)}{u(t)-u(0)} \tag{4.13}$$

This interpretation is rooting in the final value theorem. Using Eq. 4.13 in combination with the other two relation one is able to compute all needed parameters.
The system of equations as described above are called area-based methods, FEDELE, with regards to its visualization displayed in Fig. . Another, likewise valid understanding is given as the minimization of the integral of the error between the real system and the model over time.

However, the algorithm described above is not robust. It only converges iff the systems gain is equivalent with the infitity norm of the output. This resembles a dominant steady state gain. In other words, the integral Eq. 4.11 must be positive definite. To ensure this, several options are avaible.

Since a conservative estimation of the system will result in a robust controller, the gain is preferred to be calculated to big. Likewise a smaller phase increases the immunity to disturbance. Hence, a conservative bound is established with truncating the data so that the maximum output is corresponding to the end of measurement. The systems gain will be computed as

$$\hat{K} = \lim_{t\mapsto t^*} \frac{y(t^*)-y(0)}{u(\infty)-u(0)},\; y(t^*) = \sup_{0\le t\le\infty} y(t) \tag{4.14}$$

Eq. 4.14 defines the gain as the ratio between the supremum of the measurement data and the change in input. This results in a positive semidefiniteness of the integral given by Eq.4.11. Furthermore, the results in two extreme cases. The algorithm can provide the real system, iff the output data is monotonically increasing. With that, the supremum of the collected data is equal to the final value and Eq.4.14 converges to Eq. 4.13. On the other hand the system is identified as a (scaled) step response or a strictly proportional element, iff the supremum is equal to the first collected data point. An illustration of the former reasoning is given in FIGURE.

4.3 Asymmetric Relay Experiment

Another class of experimental methods based on a priori model structure is called relay experiments. These methods have been introduced in the early 1980's, ASTROEMHAGGALUND1983, and have since then been investigated, developed and used in an industrial context, see REFEREZEN. The following section is mainly based on the recent works BERNER I, II und III.

The key concept to estimate the needed parameters is based on the systems response to an (asymmetric) relay input, forcing a semi-stationary limit cylce. This behaviour is illustrated in FIG. .

HIER FIGURE

The block diagram used to generate the output is shown in FIG.

HIER FIGURE

The relay generating the input signal of the process can be described as follows:

$$u(t) = \begin{cases} u_H & e(t) > h,\ \dot{e}(t) > 0 \\ u_H & e(t) < h,\ \dot{e}(t) < 0 \\ u_L & e(t) > -h,\ \dot{e}(t) > 0 \\ u_L & e(t) < -h,\ \dot{e}(t) < 0 \end{cases} \tag{4.15}$$

In Eq. 4.15 the output switches between an upper and lower limit, $u_H, u_L \in \mathbb{R}, u_H \geq u_L$ depending on the hysterises $h \in \mathbb{R}^+$, the error of the signal and its time derivative. Iff the relation $|u_H \ = |u_L$ holds true, the relay is called symmetric, if not it is an asymmetric relay, with $|u_H \ > |u_L$. Note that the system of equations above can be formulated with respect to the former value of itsself. Since the process is defined around a set point $y_R \in \mathbb{R}$ it is usefull to define the corresponding input $u_R \in \mathbb{R}|y = y_R$. Hence, the difference in input is given by $\delta u_H = |u_H - u_R|$ and $\delta u_L = |u_L - u_R|$.

From FIG a difference the period $t_P = t_{on} + t_{off} \in \mathbb{R}^+$ consiting of the sum of the half-periods $t_{on} \in \mathbb{R}^+|u = u_H$ and $t_{off} \in \mathbb{R}^+|u = u_L$.

To estimate the parameter set of a FOTD model, the normalized time delay is approximated according to BERNER2015:

$$
\begin{aligned}
\tau &= \frac{\hat{L}}{\hat{T} + \hat{L}} \\
&= \frac{\gamma - \rho}{(\gamma - 1)\,(0.35\,\rho + 0.65)}
\end{aligned}
\tag{4.16}
$$

With the half-period ratio $\rho = \frac{\max(t_{on}, t_{off})}{\min(t_{on}, t_{off})} \in \mathbb{R}^+$ and $\gamma = \frac{\max(\delta u_H, \delta u_L)}{\max(\delta u_H, \delta u_L)}$ being the asymmetry level of the relay. Notice the impact of an symmetry in the relay, since it immediatly follows that Eq. 4.16 is singular if the amplitudes are symmetric. Furthermore, the delay is zero estimated to zero iff the half-period ratio is equal to the asymmetry level.

To compute the gain the following relationship can be utilized:

$$
\begin{aligned}
\hat{K} &= \frac{\int_{t_P} y(t) - y_R \; dt}{\int_{t_P} u(t) - u_R \; dt} \\
&= \frac{\int_{t_P} y(t) - y_R \; dt}{\int_{t_P} (u_H - u_R)\; t_{on} - (u_L - u_R)\; t_{off}}
\end{aligned}
\tag{4.17}
$$

Eq. 4.17 calculates the gain as a ratio between the quasi stationary limit cycles. The importance of the asymmetry is again visible by investigating the denominator. Singularities of Eq. 4.17 are given iff the quantities of turn-on and turn-off phase are either equal, which resembles a symmetric relay, or in a suitable ratio to each other.

The time constant of the model can be calculated using one of the following equations:

$$
\begin{aligned}
t_{on} &= \hat{T}\; \log\left(\frac{h/\hat{K} - \delta u_L + e^{\frac{\hat{L}}{\hat{T}}}\,(\delta u_H + \delta u_L)}{\delta u_H - h/\hat{K}}\right) \\
t_{off} &= \hat{T}\; \log\left(\frac{h/\hat{K} - \delta u_H + e^{\frac{\hat{L}}{\hat{T}}}\,(\delta u_H + \delta u_L)}{\delta u_L - h/\hat{K}}\right)
\end{aligned}
\tag{4.18}
$$

Eq. 4.18 can be exploited by using the Eq. 4.16 by solving it for the ratio between time delay and time constant. Hence, the system can be used to computed $\hat{T}$ and thus $\hat{L}$.

4.4 Review

Above two important and well known fitting techniques based on structural knowledge and hence mathematical formulations of the model have been introduced. Even though both methods are used throughout industry, there are certain drawbacks to each method which should be considered.

5 Multivariable Controller Design

The controller design can be divided into the SISO design process for a single controller and the MIMO design process for the interconnected system. Both tasks are equally important and are studied extensively throughout literature, see e.g. [4].

5.1 AMIGO Tuning Rules

Explain MIGO and AMIGO.
Explain Tuning

5.2 Relative Gain Array

Bristols RGA

5.3 Decoupling of Multivariable Processes

Decoupling Control proposed by Astrom et.al.

A method for the design of decoupling controllers is proposed in [6] and [**?**]. It designs a controller which limits the interaction near the steady state of the plant. To achieve this behaviour a decoupler $\boldsymbol{D} \in \mathbb{R}^{n_y \times n_y}$ is introduced. A static decoupling is proposed such that $\boldsymbol{D} = \boldsymbol{G}^{-1}|_{s=0}$ that transforms the system with the mapping $\boldsymbol{G}\boldsymbol{D} = \boldsymbol{G}^* \in \mathbb{R}^{n_y \times n_y}$. The resulting closed loop is then given by:

$$\begin{aligned} \boldsymbol{H} &= \left[\boldsymbol{I} - \boldsymbol{G}\boldsymbol{D}\boldsymbol{K}_y^*\right]^{-1} \boldsymbol{G}\boldsymbol{D}\boldsymbol{K}_r^* \\ &= \left[\boldsymbol{I} - \boldsymbol{G}^*\boldsymbol{K}_y^*\right]^{-1} \boldsymbol{G}^*\boldsymbol{K}_r^* \\ &= \left[\boldsymbol{I} - \boldsymbol{G}\boldsymbol{K}_y\right]^{-1} \boldsymbol{G}\boldsymbol{K}_r \end{aligned} \tag{5.1}$$

Eq. 5.1 gives various important transformations between the controller and system of the original identified system and the new transformed system.

A Taylor series around the steady state of the transformed system is given by:

$$\begin{aligned} \boldsymbol{G}^* &= \sum_{i=0}^{\infty} \frac{d^i}{ds^i} \boldsymbol{G}^*|_{s=0} \frac{s}{i!} \\ &= \boldsymbol{I} + s\boldsymbol{\Gamma}^* + \mathcal{O}\left(s^2\right) \\ &\approx \boldsymbol{I} + \boldsymbol{\Gamma}^* s \\ &\approx \boldsymbol{I} + \left(\boldsymbol{\Gamma}_D^* + \boldsymbol{\Gamma}_A^*\right) s \end{aligned} \tag{5.2}$$

In Eq.5.2 the coupling for small frequencies can be described via the coupling matrix $\boldsymbol{\Gamma}^* = \left(\gamma_{ij}^*\right) \in \mathbb{R}^{n_y \times n_y}$. The matrix consists both of diagonal and anti diagonal entries $\boldsymbol{\Gamma}^* = \boldsymbol{\Gamma}_D^* + \boldsymbol{\Gamma}_A^*$ which describe the small signal behaviour in an adequate way.

Substitute Eq.5.2 in the numertator of Eq. 5.1 holds:

$$\begin{aligned} \boldsymbol{H} &\approx \left[\boldsymbol{I} - \boldsymbol{G}^* \boldsymbol{K}_y^*\right]^{-1} \left[\boldsymbol{I} + \boldsymbol{\Gamma}^* s\right] \boldsymbol{K}_r^* \\ &\approx \left[\boldsymbol{I} - \boldsymbol{G}^* \boldsymbol{K}_y^*\right]^{-1} \left[\boldsymbol{I} + \left(\boldsymbol{\Gamma}_D^* + \boldsymbol{\Gamma}_A^*\right) s\right] \boldsymbol{K}_r^* \end{aligned} \tag{5.3}$$

The anti diagonal entries are given by

$$\boldsymbol{H}_A \approx \left[\boldsymbol{I} - \boldsymbol{G}^* \boldsymbol{K}_y^*\right]^{-1} \left[\boldsymbol{\Gamma}_A^* s\right] \boldsymbol{K}_r^* \tag{5.4}$$

Which is simplified according to AstrÃ¶m Paper to:

$$|h_{ij}| = \left| \left(\prod_{k=1}^{i} S_k^* \right) \gamma_{ij}^* s \, k_{r,jj}^* \right| \tag{5.5}$$

Where $k_{r,jj}^*$ is the j-th entry of the diagonal controller used for the reference signal $\boldsymbol{K}_r^*$. Eq. 5.5 can be used to describe a decoupling of the controller by using an upper limit $h_{ij,max}^* \geq |h_{ij}^*| \in \mathbb{R}^+$ which describes the maximal allowed or desired interaction between the j-th input and the i-th output. For the special case where $k_{r,jj}^*$ is a pure integrator $k_{r,jj}^* = \frac{k_{I,jj}^*}{s}$ Eq. 5.5 becomes:

$$\begin{aligned} |h_{ij}| &= \left| \left(\prod_k S_k^* \right) \gamma_{ij}^* \, k_{I,jj}^* \right| \\ &\leq \left| \left(\prod_k M_{S,k}^* \right) \gamma_{ij}^* \, k_{I,jj}^* \right| \\ &\leq \left| h_{ij,max} \right| \end{aligned} \tag{5.6}$$

The relation given by Eq. 5.6 gives a condition for detuning a purely integral controller. Since not every controller is given in this form, the structure is extended to PI control by:

$$\begin{aligned} |h_{ij}| &\leq \left| \left(\prod_k M_{S,k} \right) \gamma_{ij}^* s \left(k_{P,jj}^* + k_{I,jj}^* \frac{1}{s} \right) \right| \\ &\leq \left| \left(\prod_k M_{S,k} \right) \gamma_{ij}^* \right| \left| \left(k_{P,jj}^* s + k_{I,jj}^* \right) \right| \\ &\leq \left| \left(\prod_k M_{S,k} \right) \gamma_{ij}^* \right| \left| \left(k_{P,jj}^* j\omega + k_{I,jj}^* \right) \right| \\ &\leq \left| \left(\prod_k M_{S,k} \right) \gamma_{ij}^* \right| \sqrt{\left(k_{P,jj}^* \omega \right)^2 + \left(k_{I,jj}^* \right)^2} \end{aligned} \tag{5.7}$$

In Eq.5.7 the influence of the proportional controller is increasing with the frequency. To detune the controller sufficiently, an adequate frequency must be chosen. For a small signal interpretation $\omega \ll 1$ a detuning for just the integral gain is acceptable.

In [?, p.172 f.] the crossover frequency of a transfer function is limited by an upper bound

$$\omega_C \leq \frac{1}{L} \tag{5.8}$$

Hence, an appropriate conservative boundary can be established with the minimum time delay of the system $L_{Min} | L \geq L_{Min} \forall L \in \Sigma$ to be:

$$|h_{ij}| \leq \left| \left(\prod_k M_{S,k} \right) \gamma_{ij}^* \right| \sqrt{ \left(\frac{k_{P,jj}^*}{L_{Min}} \right)^2 + \left(k_{I,jj}^* \right)^2 } \tag{5.9}$$

Both Eq. 5.6 and 5.9 can be rewritten with a matrix $\boldsymbol{H}_{Max} = \left(h_{ij,Max} \right) \in \mathbb{R}^{n \times n}$ and the matrix of the maximum sensitivities of the diagonal transfer functions $\boldsymbol{M}_S^* = \left(M_{S,i}^* \right) \in \mathbb{R}^{n \times n}$. Using the definition of the maximum sensitivity matrix as diagonal, one can rewrite $\prod_k M_{S,k}^* = \det(\boldsymbol{M}_S)$. Once again dividing into a diagonal and anti diagonal matrix holds:

$$\boldsymbol{H}_{A,max} \geq \det(\boldsymbol{M}_S^*) \boldsymbol{\Gamma}_A^* \boldsymbol{K}_r^* \tag{5.10}$$

The method proposed above gives many advantages over a controller design based on RGA while holding the number of controllers minimal. The enhancement of performance comes through the interconnection of the controller outputs via the decoupler, which can be viewed as a simple form of model based control. Whilst giving major performance improvements, the presented method has a significant disadvantages.

Depending on the model chosen for identification and the values of the coefficients, the resulting transfer function will in general be of other form than the initial identified model. Hence, algorithms depending on these models to design controllers can not be used naturally, but have to use a simplified or approximated model. This process results in a higher model error and thus in poor performance and robustness of the derived controller.

Modified Controller Design Based on Astrom et.al.

Because of these major penalties, a modified decoupling scheme is proposed. Essentially another interpretation of the equations given above leds to a more physical meaningful design process. At first, diagonal and anti-diagonal entries of a matrix multiplication are reviewed:

$$\begin{aligned} \boldsymbol{G}^A \boldsymbol{G}^B &= \begin{bmatrix} \boldsymbol{G}_{11}^A & \boldsymbol{G}_{12}^A \\ \boldsymbol{G}_{21}^A & \boldsymbol{G}_{22}^A \end{bmatrix} \begin{bmatrix} \boldsymbol{G}_{11}^B & \boldsymbol{G}_{12}^B \\ \boldsymbol{G}_{21}^B & \boldsymbol{G}_{22}^B \end{bmatrix} \\ &= \begin{bmatrix} \boldsymbol{G}_{11}^A \boldsymbol{G}_{11}^B + \boldsymbol{G}_{12}^A \boldsymbol{G}_{21}^B & \boldsymbol{G}_{11}^A \boldsymbol{G}_{12}^B + \boldsymbol{G}_{12}^A \boldsymbol{G}_{22}^B \\ \boldsymbol{G}_{21}^A \boldsymbol{G}_{11}^B + \boldsymbol{G}_{22}^A \boldsymbol{G}_{21}^B & \boldsymbol{G}_{21}^A \boldsymbol{G}_{12}^B + \boldsymbol{G}_{22}^A \boldsymbol{G}_{22}^B \end{bmatrix} \end{aligned} \tag{5.11}$$

Eq. 5.11 states that the diagonal entries relate to either pure diagonal or pure anti-diagonal entries of the factors. Anti-diagonal entries are always the mixed product of diagonal and anti-diagonal terms.

Starting with Eq. 5.1 diagonal and antidiagonal entries of the numerator can be identified:

$$\begin{aligned} \boldsymbol{D}\boldsymbol{K}^* &= \boldsymbol{K} \\ (\boldsymbol{D}_D + \boldsymbol{D}_A)\,\boldsymbol{K}^* &= (\boldsymbol{K}_D + \boldsymbol{K}_A) \\ (\boldsymbol{D}_D + \boldsymbol{D}_A)\,\boldsymbol{D}^{-1}\boldsymbol{K} &= (\boldsymbol{K}_D + \boldsymbol{K}_A) \end{aligned} \tag{5.12}$$

Eq. 5.12 relates the diagonal controller $\boldsymbol{K}_D \in \mathbb{C}^{n \times n}$ designed via the diagonal transfer functions g_{ii} to the decoupling controller proposed by Aström et.al.. Since $\boldsymbol{K}^*$ is diagonal a direct relationship between the antidiagonal elements of the controller can be established:

$$\begin{aligned} \boldsymbol{K}_A &= \boldsymbol{D}_A\boldsymbol{K}^* \\ &= \boldsymbol{D}_A D^{-1}\,(\boldsymbol{K}_D + \boldsymbol{K}_A) \end{aligned}$$

Which is able to relate the diagonal and antidiagonal controller to each other:

$$\begin{aligned} \boldsymbol{K}_A &= \left[\boldsymbol{I} - \boldsymbol{D}_A\boldsymbol{D}^{-1}\right]^{-1}\boldsymbol{D}_A\boldsymbol{D}^{-1}\boldsymbol{K}_D \\ &= \left[\boldsymbol{D}\boldsymbol{D}_D^{-1} - \boldsymbol{I}\right]\boldsymbol{K}_D \\ &= \boldsymbol{D}_A\boldsymbol{D}_D^{-1}\boldsymbol{K}_D \\ &= \boldsymbol{\Sigma}\boldsymbol{K}_D \end{aligned} \tag{5.13}$$

Eq. 5.13 defines the splitter $\boldsymbol{\Sigma} \in \mathbb{R}^{n \times n}$ which can substitute the antidiagonal controller in Eq.5.12:

$$\boldsymbol{D}\boldsymbol{K}^* = [\boldsymbol{I} + \boldsymbol{\Sigma}]\,\boldsymbol{K}_D \tag{5.14}$$

An interesting property of the splitter is the intuitive relation between the main diagonal entries of the system and the anti diagonal entries. Since we can invert a block sufficient conditioned block matrix via:

$$\begin{bmatrix} \boldsymbol{G}_{11} & \boldsymbol{G}_{12} \\ \boldsymbol{G}_{21} & \boldsymbol{G}_{22} \end{bmatrix}^{-1} = \begin{bmatrix} \left[\boldsymbol{G}_{11} - \boldsymbol{G}_{12}\boldsymbol{G}_{22}^{-1}\boldsymbol{G}_{22}\right]^{-1} & -\boldsymbol{G}_{11}^{-1}\boldsymbol{G}_{12}\left[\boldsymbol{G}_{22} - \boldsymbol{G}_{21}\boldsymbol{G}_{11}^{-1}\boldsymbol{G}_{12}\right]^{-1} \\ -\boldsymbol{G}_{22}^{-1}\boldsymbol{G}_{21}\left[\boldsymbol{G}_{11} - \boldsymbol{G}_{12}\boldsymbol{G}_{22}^{-1}\boldsymbol{G}_{21}\right]^{-1} & \left[\boldsymbol{G}_{22} - \boldsymbol{G}_{12}\boldsymbol{G}_{11}^{-1}\boldsymbol{G}_{12}\right]^{-1} \end{bmatrix} \tag{5.15}$$

The splitter given by $\boldsymbol{D}_A\boldsymbol{D}_D^{-1}$ becomes in the notation above

$$\boldsymbol{\Sigma} = \begin{bmatrix} 0 & -\boldsymbol{G}_{11}^{-1}\boldsymbol{G}_{12} \\ -\boldsymbol{G}_{22}^{-1}\boldsymbol{G}_{21} & 0 \end{bmatrix} \tag{5.16}$$

It is clearly visible that the splitter weights the minor with the main diagonals. It can be connected both to feedforward control and disturbance rejection by dividing the system as shown in FIGURE.

Investigating the relationship between the diagonal Sensitivity of the transformed System and the ideal Sensitivities of the Diagonal system holds:

$$\begin{aligned} S^* &= \left[\boldsymbol{I} + \boldsymbol{G}\left[\boldsymbol{I} + \boldsymbol{\Sigma}\right]\boldsymbol{K}_D\right]_D^{-1} \\ &= \left[\boldsymbol{I} + \boldsymbol{G}_D\boldsymbol{K}_D + \boldsymbol{G}_A\boldsymbol{\Sigma}\boldsymbol{K}_D\right]^{-1} \\ &= \left[\boldsymbol{S}^{-1} + \boldsymbol{\Delta}_S\right]^{-1} \end{aligned} \tag{5.17}$$

Eq. 5.17 states that the transformed sensitivity is not equal to the sensitivity of the main diagonal system. Instead an error $\boldsymbol{\Delta}_S \in \mathbb{C}^{n\times n}$ relating to the influence of the anti diagonal entries via feedback is formed. From Eq. 5.17 follows directly

$$\begin{aligned} \boldsymbol{S} &= \left[\boldsymbol{S}^{-*} - \boldsymbol{\Delta}_S\right]^{-1} \\ &= \left[\boldsymbol{S}^{-*}\left[\boldsymbol{I} - \boldsymbol{S}^{-*}\boldsymbol{\Delta}_S\right]\right]^{-1} \\ &= \left[\boldsymbol{I} - \boldsymbol{S}^{-*}\boldsymbol{\Delta}_S\right]^{-1}\boldsymbol{S}^* \end{aligned} \tag{5.18}$$

Eq. 5.18 states equivalently

$$\begin{aligned} \boldsymbol{M}_S &\geq \boldsymbol{S} \\ &\geq \left[\boldsymbol{I} - \boldsymbol{S}^{-*}\boldsymbol{\Delta}_S\right]^{-1}\boldsymbol{S}^* \end{aligned} \tag{5.19}$$

Eq. 5.19 describes the transformation between the Maximum Sensitivities. Using the Triangle inequality holds:

$$\begin{aligned} \left[\left|\boldsymbol{I} - \boldsymbol{S}^{-*}\boldsymbol{\Delta}_S\right|\right]^{-1} &\geq \left[\boldsymbol{I} + \left|\boldsymbol{S}^{-*}\right|\left|\boldsymbol{\Delta}_S\right|\right]^{-1} \\ &\geq \left[\boldsymbol{I} + \boldsymbol{M}_S^{-*}\left|\boldsymbol{\Delta}_S\right|\right]^{-1} \end{aligned} \tag{5.20}$$

Hence, a conservative lower and upper bound can be defined:

$$\left[\boldsymbol{I} + \boldsymbol{M}_S^{-*}\min_{\omega}\left|\boldsymbol{\Delta}_S\right|\right]^{-1}\boldsymbol{M}_S^* \leq \boldsymbol{M}_S \leq \left[\boldsymbol{I} + \boldsymbol{M}_S^{-*}\max_{\omega}\left|\boldsymbol{\Delta}_S\right|\right]^{-1}\boldsymbol{M}_S^* \tag{5.21}$$

The lower boundary represents a conservative transformation. The most conservative transform is given by $\boldsymbol{\Delta}_S = \boldsymbol{0}$. This resembles the fact that the magnitude of superpositioned transfer functions is less or equal to the sum of its magnitudes. Hence, the most conservative approximation is given by assuming the system is equal to its transformed system.

To detune the controller the anti diagonal parts of the transfer function are used. Explicitly the term is given by

$$\begin{aligned}\boldsymbol{\Gamma}_A &= \left[\frac{d}{ds}\left[\boldsymbol{G}\left[\boldsymbol{I}+\boldsymbol{\Sigma}\right]\right]|_{s=0}\right]_A \\ &= \frac{d}{ds}\left[\boldsymbol{G}_A + \boldsymbol{G}_D\boldsymbol{\Sigma}\right]|_{s=0}\end{aligned} \tag{5.22}$$

With the maximum allowed interaction and sensitivities the detuning formula is given by:

$$\begin{aligned}\boldsymbol{H}_{A,Max} &\geq \boldsymbol{M}_S\boldsymbol{\Gamma}_A\boldsymbol{K}_r \\ &\geq \det(\boldsymbol{M}_S)\boldsymbol{\Gamma}_A\boldsymbol{K}_r\end{aligned} \tag{5.23}$$

6 Control of TITO FOTD Processes

The folllowing chapter

6.1 Analytic Decoupling

Since a FOTD are the model structure choosen for this work a deeper investigation of transfer function matrices based on this model is performed. For the following section a simple two input two output model given as following is defined:

$$\boldsymbol{G} = \begin{bmatrix} g_{11} & g_{12} \\ g_{21} & g_{22} \end{bmatrix}, g_{ij} = \frac{K_{ij}}{T_{ij}s + 1} e^{-L_{ij}s} \tag{6.1}$$

For the system described in Eq. 6.1 three different controller based on PI-structure are defined using the methods presented in the previous chapter. Further restrictions on the systems performance are given by the Maximum Sensitivity and Maximum Interaction of the system given by:

$$\begin{aligned} \boldsymbol{H}_{A,Max} &= \begin{bmatrix} 0 & h_{12,Max} \\ h_{21,Max} & 0 \end{bmatrix} \\ \boldsymbol{M}_S &= \begin{bmatrix} M_{S,1} & 0 \\ 0 & M_{S,2} \end{bmatrix} \end{aligned} \tag{6.2}$$

Eq.6.2 is given under the assumption that only the diagonal transfer functions are requiered and the interaction acts on the antidiagonal entries. Furthermore the system will be operating near steady state and hence the frequency used for Taylor Series Exapnsion is choosen to be $s = 0$.

Controller Design via Relative Gain Array Analysis

Assuming the diagonal dominance of the system, the controller are designed via the transfer functions g_{11} and g_{22}. Since the AMIGO Algorithm has been given earlier ZITIEREN and explicit values for this example will be given later on, no further description will be given at this point.

Controller Design via Aström et. al.

At first the decoupler is designed via the inverse static gain of the system

$$\begin{aligned} \boldsymbol{D} &= \boldsymbol{G}|_{s=0}^{-1} \\ &= \frac{1}{K_{11}K_{22} - K_{12}K_{21}} \begin{bmatrix} K_{22} & -K_{21} \\ -K_{12} & K_{11} \end{bmatrix} \end{aligned} \tag{6.3}$$

And with the decoupler the transformed system $\boldsymbol{G}^*$ is calculated to be

$$
\begin{aligned}
G^* &= GD \\
&= \frac{1}{K_{11}K_{22} - K_{12}K_{21}} \begin{bmatrix} g_{11} & g_{12} \\ g_{21} & g_{22} \end{bmatrix} \begin{bmatrix} K_{22} & -K_{21} \\ -K_{12} & K_{11} \end{bmatrix} \\
&= \frac{1}{K_{11}K_{22} - K_{12}K_{21}} \begin{bmatrix} K_{22}g_{11} - K_{12}g_{12} & -K_{21}g_{11} + K_{22}g_{12} \\ K_{22}g_{21} - K_{12}g_{22} & -K_{21}g_{21} + K_{11}g_{22} \end{bmatrix}
\end{aligned}
\tag{6.4}
$$

From Eq. 6.4 it is clear that the entries g^*_{ij} are linear combinations of FOTD transfer functions. Due to the properties of the exponential function the superposition principle does not hold. Hence a controller via the AMIGO algorithm can only be designed if a sufficient approximation of the linear combination as a FOTD can be formulated:

$$
\begin{aligned}
g^*_{ij} &= \frac{K^*_{ij}}{T^*_{ij}s + 1} e^{-L^*_{ij}s} + \Delta g^*_{ij} \\
&\approx \frac{K^*_{ij}}{T^*_{ij}s + 1} e^{-L^*_{ij}s}
\end{aligned}
\tag{6.5}
$$

Within Eq. 6.5 the main drawback of the method is layed out. As stated earlier, most algorithms for PI(D) design rely on a fixed model structure and hence are not fit to process information given by a combination. To use the function, two methods are proposed.

Assuming the results of the experiment used for identifying the process are still avaible the process approximate model can be found via a weighted sum of the systems output. First the static gain of every transfer function is determined via

$$
K_{ij} = \frac{y_i(\infty) - y_i(0)}{u_j(\infty) - u_j(0)} \tag{6.6}
$$

As explained earlier. Subsequent the results of a linear combination are given by:

$$
y^*_1(t) = \frac{K_{22}y_{11}(t) - K_{12}y_{12}(t)}{\det(\boldsymbol{K})} \tag{6.7}
$$

Eq. 6.7 reuses the experimental data to approximate the systems output. y_{ii} is the i-th output of the system reacting to excitation via the i-th input. Hence the data can be used for FOTD identification as presented earlier.

The second method relies on knowledge about the behaviour of the transfer functions in the time domain. At first, the static gain is given by:

$$
K^*_{11} = \frac{K_{22}K_{11} - K^2_{12}}{\det(K)} \tag{6.8}
$$

Since the integral is a linear operator the time integral can be rewritten as:

$$
\begin{aligned}
\int_0^\infty y_1^*(\infty) - y_1^*(t)dt &= K_{11}^*(T_{11}^* + L_{11}^*) \\
&= \frac{1}{\det(K)} \left(K_{22} \int_0^\infty y_{11}(\infty) - y_{11}(t)dt + K_{12} \int_0^\infty y_{12}(\infty) - y_{12}(t)dt \right) \\
&= \frac{1}{\det(K)} \left(K_{22}K_{11}(T_{11} + L_{11}) + K_{12}^2(T_{12} + L_{12}) \right)
\end{aligned}
\tag{6.9}
$$

To determine the coefficients of the new system a third equation is needed. It is convinient to choose an appropriate value for the new time delay L^* with several options like a weighted sum, the minimum or maximum of all involved delays. A robust method is given by choosing the maximum and hence implement a conservative tuning. Subsequently Eq. 6.9 can be rearranged to

$$
T_{11}^* = \frac{1}{\det(K)K_{11}^*} \left(K_{22}K_{11}(T_{11} + L_{11}) + K_{12}^2(T_{12} + L_{12}) \right) - L_{11}^* \tag{6.10}
$$

Assuming a sufficient approximation can be found and the resulting error is minimal the diagonal controller can be designed. A choice for a PI-Structure with set point weighting $b = 0$ holds:

$$
\begin{aligned}
\boldsymbol{K}_y^* &= \begin{bmatrix} -K_{P1}^* - K_{I1}^* \frac{1}{s} & 0 \\ 0 & -K_{P2}^* - K_{I2}^* \frac{1}{s} \end{bmatrix} \\
\boldsymbol{K}_r^* &= \begin{bmatrix} K_{I1}^* \frac{1}{s} & 0 \\ 0 & K_{I2}^* \frac{1}{s} \end{bmatrix}
\end{aligned}
\tag{6.11}
$$

With parameters $K_{P,i}, K_{I,i} \in \mathbb{R}$ are calculated via the AMIGO Tuning Rules as given earlier. Since the approximation given in Eq.6.5 holds an inevitable error so do the parameter.

The coupling matrix of the antidiagonal parts is given by:

$$
\begin{aligned}
\boldsymbol{\Gamma}_A &= \left[\frac{d}{ds} \boldsymbol{G}|_{s=0}^* \right]_A s \\
&= \begin{bmatrix} 0 & \frac{-K_{21}K_{11}(T_{11}-L_{11})+K_{22}K_{12}(T_{12}-L12)}{K_{11}K_{22}-K_{12}K_{21}} \\ \frac{-K_{12}K_{22}(T_{22}-L_{22})+K_{22}K_{21}(T_{21}-L_{21})}{K_{11}K_{22}-K_{12}K_{21}} & 0 \end{bmatrix} s \\
&\approx \begin{bmatrix} 0 & K_{12}^*(T_{12}^* - L_{12}^*) \\ K_{21}^*(T_{21}^* - L_{21}^*) & 0 \end{bmatrix} s
\end{aligned}
\tag{6.12}
$$

From Eq. 6.12 the dependency of the coupling on the both the static gain of the system and the dynamical behaviour can be observed. This coincides with the statements of LUNZE ZITIEREN.

Detuning the controller requires to define both maximum allowed interactions $h_{ij,Max}$ and maximum sensitivity $M_{S,i}$ of the closed loop:

$$
\begin{aligned}
\boldsymbol{H}_{A,Max} &= \begin{bmatrix} 0 & h_{12,Max} \\ h_{21,Max} & 0 \end{bmatrix} \\
\boldsymbol{M}_S &= \begin{bmatrix} M_{S,1} & 0 \\ 0 & M_{S,2} \end{bmatrix}
\end{aligned}
$$

Solving Eq. **??** for the set point weighting controller holds:

$$
\begin{aligned}
\boldsymbol{K}_r^* &\leq \boldsymbol{\Gamma}_{A,Max}^{-*} \boldsymbol{M}_S^{-1} \boldsymbol{H}_{A,Max}^* \\
&\leq \frac{1}{\det(\boldsymbol{M}_S)} \boldsymbol{\Gamma}_{A,Max}^{-*} \boldsymbol{H}_{A,Max}^* \\
&\leq \frac{1}{M_{S,1} M_{S,2}} \begin{bmatrix} \frac{h_{21,Max}}{K_{12}^*(T_{12}^* - L_{12}^*)} & 0 \\ 0 & \frac{h_{12,Max}}{K_{21}^*(T_{21}^* - L_{21}^*)} \end{bmatrix}
\end{aligned}
\tag{6.13}
$$

Controller Design via Modified Aström

Now the modified Algorithm proposed in this thesis is applied to the same System. First, we design the controller as a function of the main diagonal entries g_{ii} once again using the AMIGO Tuning rules:

$$
\begin{aligned}
\boldsymbol{K}_y &= \begin{bmatrix} -K_{P1} - K_{I1}\frac{1}{s} & 0 \\ 0 & -K_{P2} - K_{I2}\frac{1}{s} \end{bmatrix} \\
\boldsymbol{K}_r &= \begin{bmatrix} K_{I1}\frac{1}{s} & 0 \\ 0 & K_{I2}\frac{1}{s} \end{bmatrix}
\end{aligned}
\tag{6.14}
$$

The splitter $\boldsymbol{\Sigma}$ is likewise designed by the steady state of the system as:

$$
\begin{aligned}
\boldsymbol{\Sigma} &= \boldsymbol{D}_A \boldsymbol{D}_D^{-1} \\
&= \begin{bmatrix} 0 & -\frac{K_{12}}{K_{11}} \\ -\frac{K_{21}}{K_{22}} & 0 \end{bmatrix}
\end{aligned}
\tag{6.15}
$$

To test for interaction define the maximum interaction and the sensitivity like in Eq. FEHLT. The anti diagonal parts of the Taylor series can be identified as:

$$
\begin{aligned}
\boldsymbol{\Gamma}_A &= \frac{d}{ds}\left[\boldsymbol{G}_A + \boldsymbol{G}_D \boldsymbol{\Sigma}\right]|_{s=0} \\
&= \begin{bmatrix} 0 & K_{12}(T_{12} - L_{12}) - K_{11}\frac{K_{12}}{K_{11}}(T_{11} - L_{11}) \\ K_{21}(T_{21} - L_{21}) - K_{22}\frac{K_{21}}{K_{22}}(T_{22} - L_{22}) & 0 \end{bmatrix} \\
&= \begin{bmatrix} 0 & K_{12}(T_{12} - L_{12} - T_{11} + L_{11}) \\ K_{21}(T_{21} - L_{21} - T_{22} + L_{22}) & 0 \end{bmatrix}
\end{aligned}
\tag{6.16}
$$

To detune the controller solving Eq. ?? for the integral controller as before holds:

$$\begin{aligned} \boldsymbol{K}_I &\leq \boldsymbol{\Gamma}_A^{-1} \boldsymbol{M}_S^{-1} \boldsymbol{H}_{A,Max} \\ &\leq \frac{1}{\det(\boldsymbol{M}_S)} \boldsymbol{\Gamma}_A^{-1} \boldsymbol{H}_{A,Max} \\ &\leq \frac{1}{M_{S,1} M_{S,2}} \begin{bmatrix} \frac{h_{12,Max}}{K_{12}(T_{12}-L_{12}-T_{11}+L_{11})} & 0 \\ 0 & \frac{h_{21,Max}}{K_{21}(T_{21}-L_{21}-T_{22}+L_{22})} \end{bmatrix} \end{aligned} \tag{6.17}$$

6.2 Rosenbrook

Roosenbrooks function as an Example!

6.3 Woodberry

Woodberry Destillation Column as Example!

6.4 Identified System at WP 1

Working point 1

6.5 Identified System at WP 2

Working point 2

6.6 Performance Review

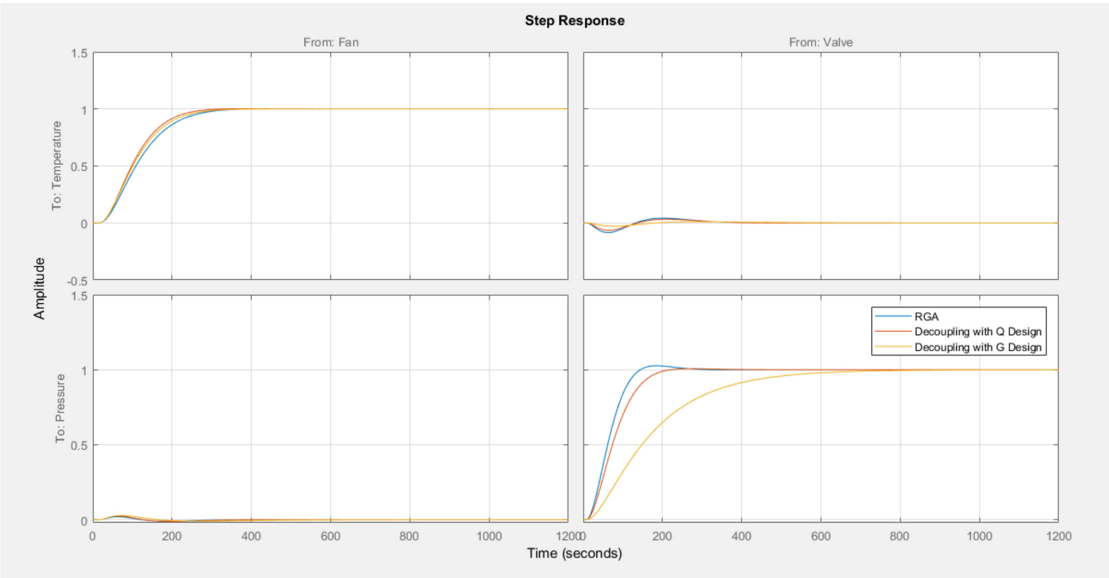

Figure 6.1: Step of the MIMO

7 Robustness Study Using Monte Carlo Methods

Monte Carlo Method explained –> Statisitical Approcach etc.

7.1 Definition of Parameter Boundaries

Statistical Exploration of the Data from System Identification!

7.2 Robustness of SISO Systems

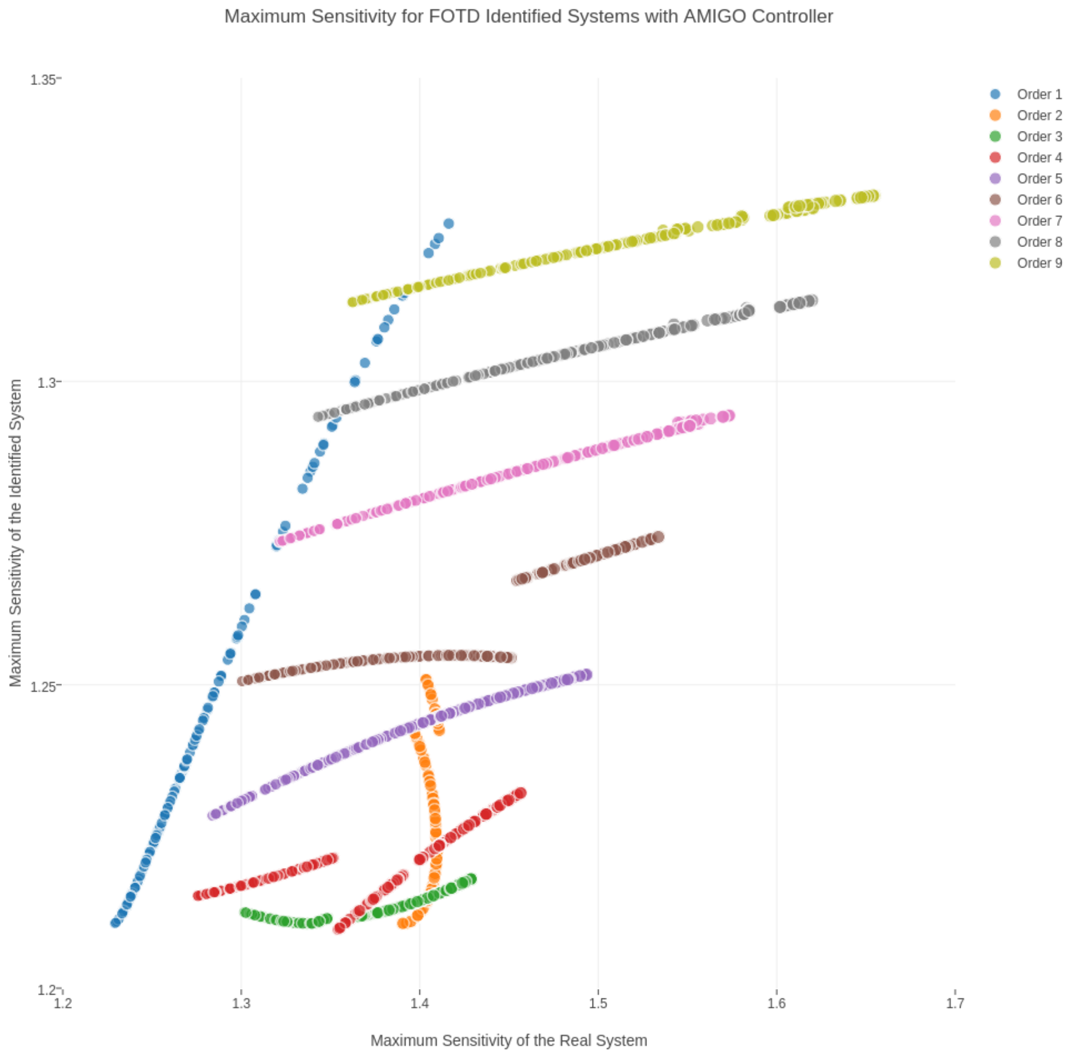

Figure 7.1: Results of the Robustness Study, Maximum Sensitivity of the Real System and the Identified System

7.3 Robustness of MIMO Systems

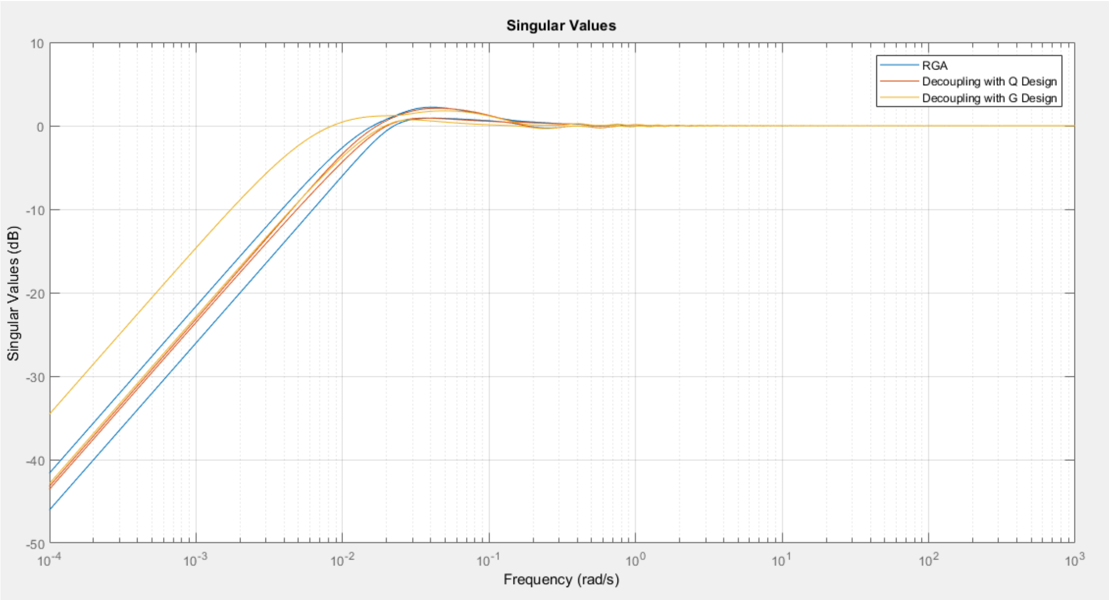

Figure 7.2: Robusteness of the MIMO

8 Application to Physical Process Models

9 Conclusion and Outlook

Bibliography

[1] ADAMY, J.: *Nichtlineare Systeme und Regelungen*. Springer Berlin Heidelberg. – 626 S. http://dx.doi.org/10.1007/978-3-642-45013-6. http://dx.doi.org/10.1007/978-3-642-45013-6. – ISBN 978–3–642–45012–9

[2] AÌŠSTROÌM, K. J. K. J.; HAÌGGLUND, T.; AÌŠSTROÌM, K. J. K. J.: *PID controllers*. International Society for Measurement and Control https://ww2.isa.org/store/products/product-detail/?productId=116103. – ISBN 9781556175169

[3] ASTRÖM, K. J.; MURRAY, R. M.: Feedback Systems An Introduction for Scientists and Engineers. (2009). http://press.princeton.edu/titles/8701.html.

[4] ÅSTRÖM, K.: Limitations on Control System Performance. In: *Eur. J. Control* 6 (2000), jan, Nr. 1, 2–20. http://dx.doi.org/10.1016/S0947-3580(00)70906-X. – DOI 10.1016/S0947–3580(00)70906–X. – ISSN 09473580

[5] ÅSTRÖM, K.; HÄGGLUND, T.; AÌŠSTROÌM, K. J. K. J.; HAÌGGLUND, T.: *Advanced PID control*. ISA-The Instrumentation, Systems, and Automation Society. – 460 S. http://lup.lub.lu.se/record/535630. – ISBN 1556179421

[6] ASTROM, K.; JOHANSSON, K.: Design of decoupled PID controllers for MIMO systems. In: *Control Conf. 2001 ...* (2001). http://ieeexplore.ieee.org/abstract/document/946038/

[7] ÅSTRÖM, K.; WITTENMARK, B.: On self tuning regulators. In: *Automatica* 9 (1973), mar, Nr. 2, 185–199. http://dx.doi.org/10.1016/0005-1098(73)90073-3. – DOI 10.1016/0005–1098(73)90073–3. – ISSN 00051098

[8] FEDELE, G.: A new method to estimate a first-order plus time delay model from step response. In: *J. Franklin Inst.* (2009). http://s3.amazonaws.com/academia.edu.documents/41626596/A{_}new{_}method{_}to{_}estimate{_}a{_}first-order{_}p20160127-1753-sogvnl.pdf?AWSAccessKeyId=AKIAIWOWYYGZ2Y53UL3A{&}Expires=1494916663{&}Signature=pAvbvKu2oGpo2{%}252BSoKdGWZcjQL6E{%}253D{&}response-content-disposition=inl

[9] LUNZE, J.: *Regelungstechnik 2*. Springer Berlin Heidelberg (Springer-Lehrbuch). http://dx.doi.org/10.1007/978-3-642-53944-2. http://dx.doi.org/10.1007/978-3-642-53944-2. – ISBN 978–3–642–53943–5

[10] LUNZE, J.: *Regelungstechnik 1*. Springer Berlin Heidelberg. http://dx.doi.org/10.1007/978-3-662-52678-1. http://dx.doi.org/10.1007/978-3-662-52678-1. – ISBN 978–3–662–52677–4

[11] Struchtrup, H. : *Thermodynamics and Energy Conversion*. Springer Berlin Heidelberg. http://dx.doi.org/10.1007/978-3-662-43715-5. http://dx.doi.org/10.1007/978-3-662-43715-5. – ISBN 978–3–662–43714–8

[12] Weigand, B. ; Köhler, J. ; Wolfersdorf, J. von: *Thermodynamik kompakt*. Springer Berlin Heidelberg (Springer-Lehrbuch). http://dx.doi.org/10.1007/978-3-642-37233-9. http://dx.doi.org/10.1007/978-3-642-37233-9. – ISBN 978–3–642–37232–2

[13] Zhou, K. ; Doyle, J. C.: *Essentials of robust control*. Prentice Hall. – 411 S. https://www.ece.lsu.edu/kemin/essentials.htm. – ISBN 0135258332

Anhang

A.1 Erster Anhang

Ein Anhang.

A.2 Zweiter Anhang

Ein weiterer Anhang.

Technische Universitï¿½t Braunschweig
Institut fï¿½r Thermodynamik
Hans-Sommer-Strasse 5
38106 Braunschweig